Contouring using two-wavelength electronic speckle pattern interferometry employing dual-beam illuminations

H. Diao, X. Peng, Y. Zou, H. J. Tiziani, L. Chen

University of Stuttgart, Institut für Technische Optik, FRG

Contouring using two-wavelength electronic speckle pattern interferometry employing dual-beam illuminations. A new contouring technique using two-wavelength electronic speckle pattern interferometry (TWESPI) employing dual-beam illuminations is proposed. The optical rough surface is tested at a synthesized longer equivalent wavelength $\lambda_{eq} = (\lambda_1\lambda_2)/(|\lambda_1 - \lambda_2|)$ so that a variable measurement sensitivity can be achieved by changing the wavelengths λ_1 and λ_2. Therefore, this technique extents the measurement range of single-wavelength electronic speckle pattern interferometry and allows the measurement of profiles of the steeper surfaces than has preciously been possible with a single-wavelength, assuming that 2π ambiguities can be removed at equivalent wavelength λ_{eq}.

Konturing mit elektronischer Zwei-Wellenlängen-Speckle-Interferometrie mit Beleuchtung von zwei Strahlen. Es wird eine neue Konturing-Methode mit elektronischer Zwei-Wellenlängen-Speckle-Interferometrie (TWESPI) vorgeschlagen, bei der zwei Beleuchtungsstrahlen verwendet werden. Die optisch rauhe Oberfläche wird bei einer synthetischen längeren equivalenten Wellenlänge $\lambda_{eq} = \lambda_1\lambda_2/(|\lambda_1 - \lambda_2|)$ vermessen, so daß durch Änderung der Wellenlängen λ_1 und λ_2 eine variable Meßempfindlichkeit erhalten werden kann. Dadurch erweitert diese Technik den Meßbereich der Ein-Wellen-Speckle-Interferometrie und erlaubt die Vermessung von Konturen steiler Profile als bisher mit der Ein-Wellenlängenmethode möglich war. Dabei wird angenommen, daß 2π Mehrdeutigkeiten durch die äquivalente Wellenlänge λ_{eq} eliminiert werden können.

1. Introduction

Electronic speckle pattern interferometry (ESPI) has been widely used as the measurement techniques for vibration analysis, contour, deformation and displacement etc. for a long time [1]. The advantage of employing ESPI is that the intermediate photographic processing is eliminated. The live correlation fringes which are related to the shape of the test object are directly shown on TV monitor. Furthermore, it is possible to use a host computer to analyze the fringes. Some of the well known ESPI techniques for contouring and shape analysis have already been discussed in various books [2].

Recently some new techniques for contouring an object using ESPI have been reported to overcome some of the drawbacks suffered by the already existing methods. The typical examples are single-wavelength techniques with either tilting the object [3] or shifting illuminated beams [4–6] and two-wavelength technique which displays the shape difference between an object and a master [2, 7].

In this paper, we present a new contouring technique using TWESPI with dual-beam illuminations and make a detailed study on the contour phase analysis. This technique uses two different wavelengths λ_1 and λ_2 to produce a long effective equivalent wavelength λ_{eq} for contouring without a master. It extents the measurement range of single-wavelength ESPI and allows the measurement of the deeper or steeper objects than has preciously been possible with a single-wavelength techniques, assuming that 2π ambiguities can be removed at equivalent wavelength λ_{eq}. The experimental results give good proofs for our analysis.

Received December 6, 1991.

H. Diao, X. Peng, Y. Zou, H. J. Tiziani, University of Stuttgart, Institut für Technische Optik, Pfaffenwaldring 9, D-7000 Stuttgart 80.

L. Chen, Precision Instrument Department, Tianjin University, Tianjin, P. R. China.

2. Basic theories

2.1 Establishment of the mathematics model

Placed on a coordinate system XYZ shown in fig. 1(a), the optical rough surface of a test object can be described by its Z coordinate. The surface $Z(x, y)$ is a stochastic process and can be split into a deterministic macroscopic shape $Z_0(x, y)$ and a statistical microscopic deviation $h(x, y)$, therefore,

$$Z(x, y) = Z_0(x, y) + h(x, y) \tag{1}$$

where x and y are the position coordinates of the surfaces of the test object. We assume that the deterministic shape Z_0 causes a deterministic phase ϕ_d when the light is scattered from point $N(x, y, z)$ of the test object to the viewing point P on the image plane; and the statistic deviation h, a statistical phase ϕ_s. Thus the complex amplitudes of the coherent light at any given point P on the image plane from both illuminations can be expressed as

$$\begin{aligned} \tilde{U}_1(P) &= A_{s1} \exp i(\phi_{s1} + \phi_{d1}) \\ \tilde{U}_2(P) &= A_{s2} \exp i(\phi_{s2} + \phi_{d2}), \end{aligned} \tag{2}$$

respectively, where A_{s1}, A_{s2} are the random amplitudes of the speckle pattern on the image plane of both illumination beams. The intensity at the point P is then given by

$$\Gamma(P) = I_1 + I_2 + 2\sqrt{I_1 I_2}\cos[(\phi_{s1} - \phi_{s2}) + \phi_d], \tag{3}$$

where

$$\begin{aligned} I_1 &= \tilde{U}_1 \tilde{U}_1^* \\ I_2 &= U_2 \tilde{U}_2^* \\ \phi_d &= \phi_{d1} - \phi_{d2}. \end{aligned}$$

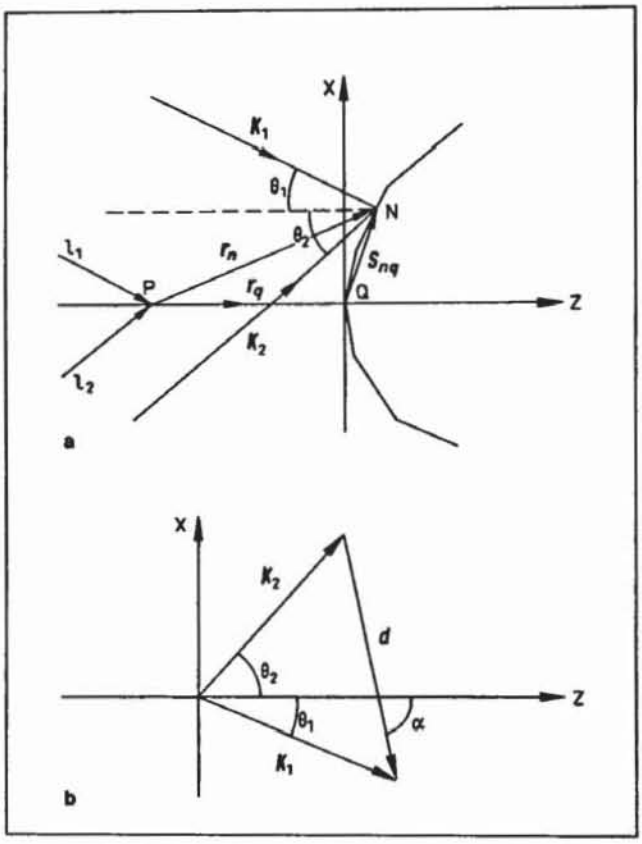

Fig. 1. a) The schematic principle geometry of contouring using TWESPI with dual-beam illuminations. b) The geometry of the illuminating vectors and the direction vector of the contour planes.

According to the geometry of fig. 1(a), the deterministic phase ϕ_{di} of the light scattered from point N to point P can be expressed as follows [6]

$$\phi_{di} = \frac{2\pi}{\lambda}(r_n + l_i + \boldsymbol{r}_n \cdot \boldsymbol{K}_i). \quad (i = 1, 2) \tag{4}$$

where the subscript i represents parameters related to the ith illumination beam; N is an arbitrary point on the test object and P is a viewing point; $\boldsymbol{r}_n$ is a position vector of point N to P and r_n is the scalar magnitude of $\boldsymbol{r}_n$; $\boldsymbol{K}_i$ is the unit direction vector of illumination beam; and λ is the wavelength of the illumination beam and l_i is the optical path of the ith illumination beam directly from the source to the viewing point P.

2.2 Theoretic analysis

In ESPI, a speckle pattern of a test object is formed on the CCD camera when the object is illuminated by a coherent light with the wavelength λ. In our experimental setups, the objects are illuminated by two beams in order that the intensity of the speckle pattern formed on the image plane is a function of the phase and of the amplitude of the light scattered from the object.

In TWESPI, a test object is first illuminated by dual-beam coherent light with wavelength λ_1. Referring to eq. (3), the distribution of the speckle pattern intensity on point P of the image plane is $\Gamma(P)$, and the phase advance can be expressed as

$$\phi_d = \frac{2\pi}{\lambda_1}[(l_1 - l_2) + \boldsymbol{r}_n \cdot (\boldsymbol{K}_1 - \boldsymbol{K}_2)]. \tag{5}$$

Then keeping the intensities of two illumination beams constant, the object is illuminated at wavelength λ_2 according to the same geometry. If the subscript ′ represents the parameters related to illuminations at a wavelength λ_2, then the distribution of the speckle pattern intensity on the point P is $\Gamma'(P)$ and the phase advance is

$$\phi'_d = \frac{2\pi}{\lambda_2}[(l'_1 - l'_2) + \boldsymbol{r}_n \cdot (\boldsymbol{K}_1 - \boldsymbol{K}_2)]. \tag{6}$$

In order to measure the object without a master, the wavelength difference $\Delta\lambda = |\lambda_1 - \lambda_2|$ is usually much smaller than the wavelength λ_1 or λ_2 so that the equivalent wavelength is long enough for removing 2π ambiguities. In our experiments, $\Delta\lambda = 0.4 \sim 0.5$ nm and $\lambda \geqq 781.66$ nm. Thus we can neglect the effect of the chromatic aberration of the optical system [7] and consider the optical paths of two illumination beams from the source to the viewing point P constant, i.e. $l_1 \cong l'_1$ and $l_2 \cong l'_2$. Eq. (6) can be written as follows

$$\phi'_d \cong \frac{2\pi}{\lambda_2}[(l_1 - l_2) + \boldsymbol{r}_n \cdot (\boldsymbol{K}_1 - \boldsymbol{K}_2)]. \tag{7}$$

Correlation between intensities Γ and Γ' can be observed by a process of video signal subtraction or addition. In the subtraction process, the CCD camera video signal corresponding to the speckle pattern intensity on the image plane is first stored electronically when the object is illuminated at wavelength λ_1, then the live video signal when the object is illuminated at a wavelength λ_2, as detected also by CCD camera, is subtracted from the stored waveform. The output with the correlation fringes is displayed on a TV monitor. If the output camera signals V_1 and V_2 are proportional to the input image intensities Γ and Γ', respectively, then the subtracted signal V_s is given by

$$\begin{aligned} V_s &= (V_1 - V_2)\,\alpha(\Gamma - \Gamma') \\ &= 4\sqrt{I_1 I_2}\sin[(\phi_{s1} - \phi_{s2}) + (\phi_d + \phi'_d)/2] \\ &\quad \cdot \sin(\psi_d/2), \end{aligned} \tag{8}$$

where $\psi_d = \phi_d - \phi'_d$.

The brightness, B, of a TV monitor is defined as [1]

$$B\,\alpha\langle(V_1 - V_2)^2\rangle^{1/2}. \tag{9}$$

After averaging the random term in eq. (9) goes to be uniform. Then

$$B\,\alpha\left(I_1 I_2 \sin^2\frac{\psi_d}{2}\right)^{1/2}, \tag{10}$$

and

$$\psi_d = C + 2\pi\left(\frac{1}{\lambda_1} - \frac{1}{\lambda_2}\right)(\boldsymbol{r}_n \cdot \boldsymbol{d})\,2\sin\left(\frac{\theta_1 + \theta_2}{2}\right), \tag{11}$$

where $\boldsymbol{d}$ is the unit difference vector of the direction vectors of both illumination beams; and

$$C = 2\pi\left(\frac{1}{\lambda_1} - \frac{1}{\lambda_2}\right)(l_1 - l_2) = \frac{2\pi}{\lambda_{eq}}(l_1 - l_2)$$

$$\boldsymbol{d} = (\boldsymbol{K}_1 - \boldsymbol{K}_2) / \left[2\sin\left(\frac{\theta_1+\theta_2}{2}\right)\right].$$

Dark correlation fringes appear when $\psi_d = 2n\pi$, where n is any integer.

2.3 Direction of contour planes

When $\boldsymbol{r}_n$ scans across the surface of a test object, the sum ψ_d on the eq. (11) passes through integral multiples of $\lambda_{eq}/\left[2\sin\left(\frac{\theta_1+\theta_2}{2}\right)\right]$, giving dark correlation loci on subtraction. If the incremental phase difference between N and Q point on the test object is $\Delta\psi_{nq}$, then [6]

$$\Delta\psi_{nq}(\boldsymbol{r}_n, \boldsymbol{r}_q, \boldsymbol{d}) = \frac{2\pi}{\lambda_{eq}}(\boldsymbol{S}_{nq}\cdot\boldsymbol{d})\, 2\sin\left(\frac{\theta_1+\theta_2}{2}\right) \tag{12}$$

where

$$\boldsymbol{S}_{nq} = \boldsymbol{r}_n - \boldsymbol{r}_q$$

where Q is the cross point between the test object and Z axis; $\boldsymbol{S}_{nq}$ is the surface position vector related to the point Q and S_{nq} is the scalar magnitude of vector $\boldsymbol{S}_{nq}$. According to eq. (12), the phase difference between the point Q and any point N on the test object can be determined by the projection of the position vector $\boldsymbol{S}_{nq}$ onto the difference vector $\boldsymbol{d}$. When taking this projection to be the value of an integral times of $\lambda_{eq}/\left[2\sin\left(\frac{\theta_1+\theta_2}{2}\right)\right]$, we obtain contour fringes. Therefore, the direction vector of the contour planes (defined as the vector normal to the contour planes) is identical with the difference vector $\boldsymbol{d}$ [4]. The inclined angle α between vector $\boldsymbol{d}$ and Z axis, as shown in fig. 1(b), may be written

$$\alpha = 90° + \tfrac{1}{2}(\theta_1 - \theta_2), \tag{13}$$

and the interval δ of the contour planes along the direction $\boldsymbol{d}$ is

$$\delta = \lambda_{eq}/\left[2\sin\left(\frac{\theta_1+\theta_2}{2}\right)\right]. \tag{14}$$

Eq. (13) and eq. (14) show the direction vector and the interval of the contour planes are related to the directions of both illuminating beams. Only when $\alpha = 0$, the direction vector $\boldsymbol{d}$ of contour planes is identical to Z axis. Referring to eq. (13), the measurement values can correctly represent the shape of the test object.

3. The design considerations of experimental set-up

Fig. 2(b) shows the vector relationships which meet the condition $\alpha = 0$ described above. The geometry is available only for transparent objects. For most of opaque objects, it is impossible to meet the condition of $\alpha = 0$. But the condition can be approached through making α value as small as possible. From eq. (13), one find α will decrease when θ_1 decreases and θ_2 increases. When two illumination beams are located on the same side of the Z axis, the direction vector of the contour planes will approach Z axis. Thus, we can get an inclined contour plane according to the geometry of fig. 4(a) which is available for the testing of an opaque object. Through the automatic calibration of the inclined contour plane by computer (introduced in another paper), we can get the correct shape of the test object.

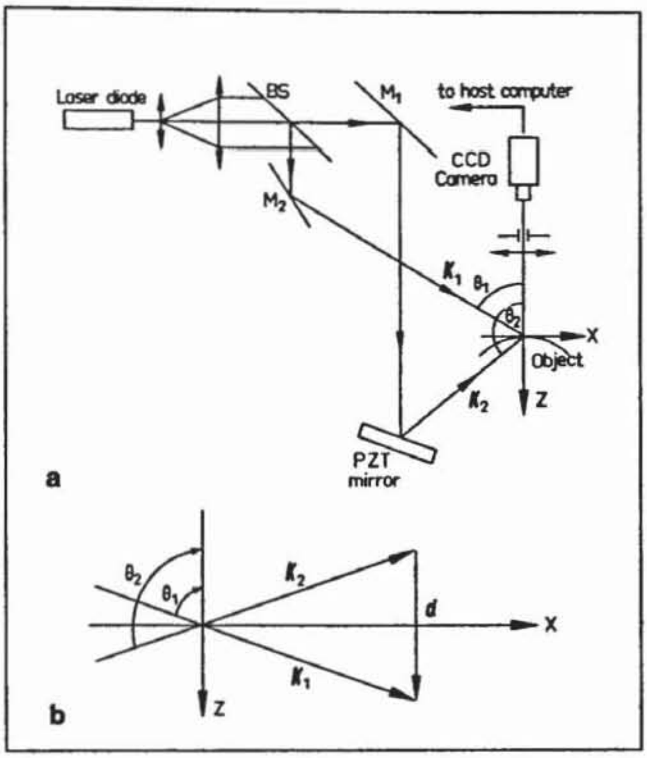

Fig. 2. a) The experimental set-up for the testing of a transparent object using TWESPI employing dual-beam illuminations. b) The vector geometry.

When two illuminating beams are located the same side of Z axis, the interval of the contour planes shown in eq. (14) can be transferred into

$$\delta = \lambda_{eq}/\left[2\sin\left(\frac{|\theta_2| - |\theta_1|}{2}\right)\right].$$

When the test object is illuminated from the same direction, the interval $\delta \to \infty$. The object can not be contoured. It is very important to select a suitable interval of the contour planes for certain test object. Therefore, the difference of the incident angles of both illumination beams has to be suitable. When $|\theta_1| > |\theta_2|$, $\delta < 0$. It means the direction vector of the contour planes reversed. The measurement values are also reversed completely so that we get the shape of the object reversed completely. Therefore, in the design of our experimental set-up, we have to consider: 1) keeping $\lambda_1 < \lambda_2$; 2) keeping the same side illuminations of the optical axis of a viewing system and $|\theta_1| + |\theta_2| \to 180°$; 3) keeping the suitable difference of the incident angles of both illuminations; 4) keeping $|\theta_1| < |\theta_2|$.

4. Experimental set-up and results

In this section, we present preliminary measurements with the technique described above. Fig. 2(a) and fig. 4(a) show the experimental set-ups which are available for the testing of a transparent object and an opaque object, respectively. We used a laser diode with 25 mW as a light source. The variation of the illuminating wavelength could be achieved by changing the temperature of the controller of laser diode. Table 1 shows the relationship between temperature and wavelength. The laser beam from laser diode was collimated and then split into two illumination beams via a beam splitter. In the optical arrangements, the objects were illuminated from the same side of the axis *Z* of the viewing system. All of the viewing system were composed of an imaging lens, an aperture and a CCD camera. The diameter of the aperture was so controlled that the averaging speckle size was set to be approximately equal to the cell size of CCD camera. First, the speckle pattern on the image plane with a wave-

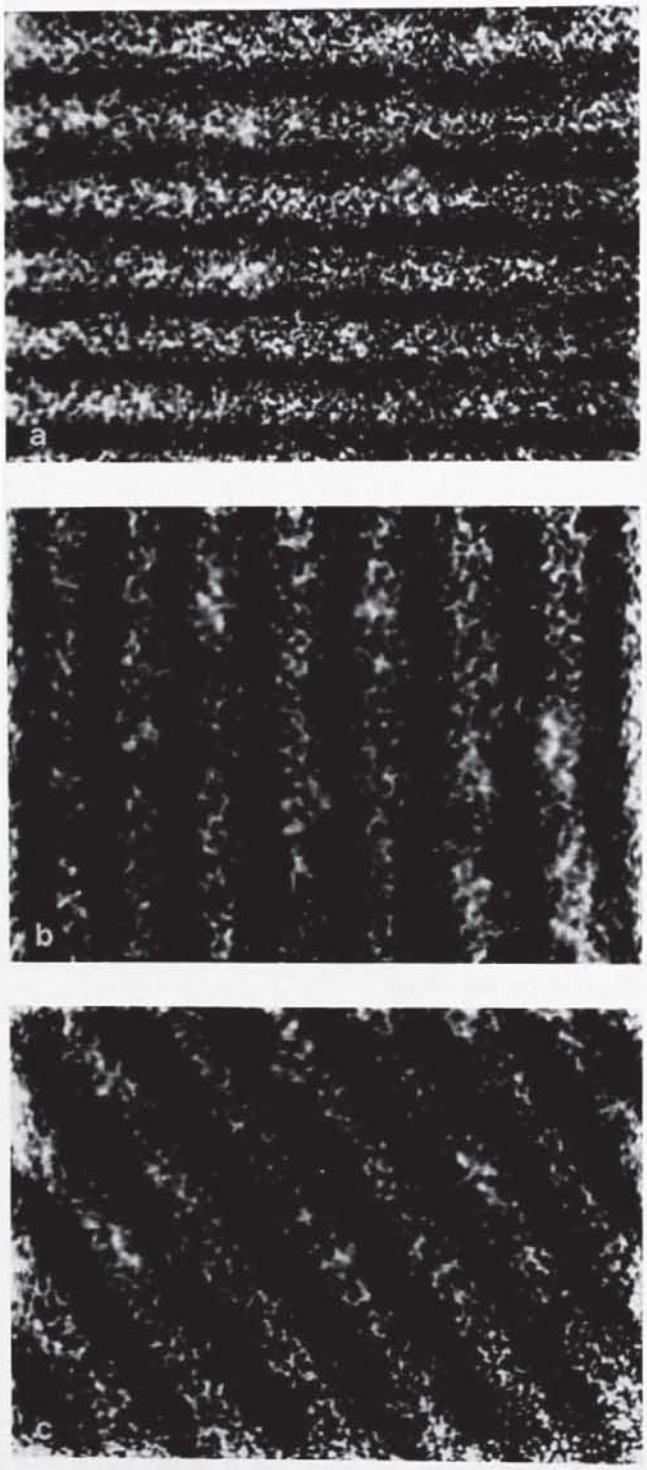

Fig. 3. The correlation fringes in fig. 2 a) arrangement when the ground glass plate (a transparent object) is located on the different orientations. a) The plate on the *XY* plane is rotated around *X* axis. b) The plate on the *XY* plane is rotated around *Y* axis. c) The plate on the *XY* plane is rotated first around *X* axis and then around *Y* axis.

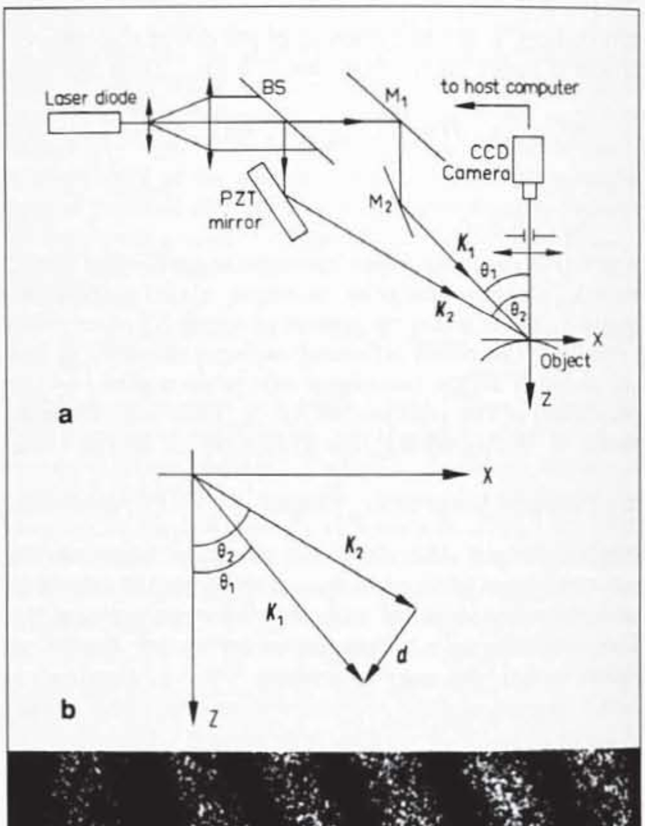

Fig. 4. a) The experimental set-up for the testing of an opaque object using TWESPI employing dual-beam illuminations. b) The vector geometry. c) The correlation fringes when the test object is a pyramid.

Table 1. Temperature vs wavelength LD head 06DLL407 + Controller LDC 700 A, constant optical power

Temperature (C)	Wavelength (nm)	Differences (nm)
20.0	781.660	
20.5	781.704	0.044
21.0	781.740	0.036
21.5	781.776	0.036
22.0	781.808	0.032
22.5	781.844	0.036
23.0	781.888	0.044
23.5	781.924	0.036
24.0	781.960	0.036
24.5	781.996	0.036
25.0	782.032	0.036
25.5	782.064	0.032
26.0	782.100	0.036
26.5	782.136	0.036
27.0	782.192	0.056
27.5	783.396	1.204

length λ_1 illumination was stored on the frame buffer or the host computer. Then we changed the wavelength λ_1 of illumination light for a wavelength λ_2. Thus, the subtracted speckle pattern was displayed on the monitor, and the contour fringe pattern related to the shape of the test object was obtained.

In the optical arrangement of fig. 2(a), $\theta_1 = -30°$, $\theta_2 = 150°$ and a ground glass plate was chosen as the test object. Selecting $\lambda_1 = 781.66$ nm and $\lambda_2 = 782.032$ nm, fig. 3(a)–(c) show the correlation fringes observed along Z axis when the plate was placed on the different orientations. In the optical arrangement of fig. 4(a), $\theta_1 \cong 0°$, $\theta_2 = 45°$ and a pyramid was chosen as the test object. Selecting $\lambda_1 = 781.66$ nm and $\lambda_2 = 782.192$ nm, the correlation fringes observed along Z were shown in fig. 4(c). The theoretical and experimental results show good agreement.

5. Conclusion

We have demonstrated a new contouring technique by using TWESPI employing dual-beam illuminations which is very valuable for the testing of steep surfaces because of the variable measurement sensitivity that can be achieved by changing the wavelengths. This technique does not need a master corresponding to the test object so that it is very convenient for the testing of the complicated shape. In TWESPI employing dual-beam illuminations, the results is noisier because of the effects of chromatic aberration and the decorrelation between two wavelengths. At the same time, the sensitivity of TWESPI is limited by the equivalent wavelength λ_{eq} used. Because the data from two wavelengths are combined, there is an error magnification in effect. In order to increase the sensitivity and the accuracy simultaneously, the single-wavelength 2π ambiguities should be removed by taking the integrated two-wavelength phase.

Acknowledgements

X. Peng, an Alexander von Humboldt fellow, would like to acknowledge the Alexander von Humboldt foundation for financial support.

The authors thank Dr. Padrini for the helpful discussion.

References

[1] J. N. Butter, C. Wykes: Electronic Speckle Pattern Interferometry. In R. K. Erf (Ed.): Speckle Metrology. Academic Press, New York 1978.

[2] R. Jones, C. Wykes: Holographic and Speckle Interferometry. Chapter 5. Camdridge U. P., London 1989.

[3] C. Joneatham, B. Pfister, H. Tiziani: Contouring by electronic speckle pattern interferometry. Appl. Opt. **29** (1990) 1905–1911.

[4] X. Peng, H. Y. Diao, Y. L . Zou, H. J. Tiziani: Contouring by modified dual-beam ESPI based on tilting illumination beams. To be published soon in Optik.

[5] Y. Zou, H. Diao, X. Peng, H. Tiziani: Geometry for Contouring by Electronic Speckle Pattern Interferometry Based on Shifting Illumination Beams. Submitted to Appl. Opt.

[6] B. D. Bergqusit, P. Montgomery: Contouring by electronic speckle pattern interferometry. Proc. SPIE **599** (1985) 189–195.

[7] K. Creath, Y. Y. Cheng, J. C. Wyant: Contouring aspheric surfaces using two-wavelength phase-shifting interferometry. Optica Acta **32** (1985) 1455–1464.